Tangential Stress-rate Effect in Soils Subjected to Cyclic Circular Stress Path in the Deviatoric Stress Plane

H. Setouchi[1], K. Hashiguchi[2], T. Shikanai[1], T. Okayasu[2]

Summary

The traditional elastoplastic constitutive equation is incapable of describing the inelastic stretching due to the stress rate tangential to the yield surface. The subloading surface model has been extended so as to describe the inelastic stretching due to the deviatoric tangential stress rate for the subloading surface. In this article, the subloading surface model is applied to the prediction of the deformation behavior of sands subjected to the cyclic loading of circular stress path in the deviatoric stress plane deviating significantly from the proportional loading. The validity is verified comparing with the test data.

Introduction

In the traditional elastoplastic constitutive equation, the plastic stretching is independent of the stress rate component tangential to the yield surface, while let the component be called the *tangential stress rate*. Therefore, the traditional formulation possesses the following defects: 1) Unrealistically stiff response is predicted for the plastic instability phenomena in which the stress path deviates from the proportional loading and thus the tangential stress rate has a significant magnitude. 2) The direction of the plastic stretching is independent of the stress rate. 3) The coaxiality, i.e. the principal axes of plastic stretching coincide with those of stress as far as an anisotropic plastic potential surface is not incorporated.

The *subloading surface model* [1] fulfills the mechanical requirements for constitutive equations, i.e. the Masing effect and the work rate-stiffness relaxation. It has been extended so as to describe the inelastic stretching due to the deviatoric tangential stress rate for the subloading surface, called the *tangential stress rate effect* [2]. It would be able to overcome the above-mentioned defects in the traditional elastoplastic constitutive equation.

In this article, in order to examine the validity of the subloading surface model with tangential stress rate effect, the simulation results are compared with the test data for the deformation behavior of sands subjected to the cyclic loading of circular stress path in the deviatoric stress plane deviating significantly from the proportional loading. The tensile stress (rate) and stretching (a symmetric component of velocity gradient) are taken to be positive throughout this article.

[1] Faculty of Agriculture, University of the Ryukyus, Nishihara,Okinawa 903-0213, JAPAN

[2] Department of Bioproduction Enviromental Sciences, Graduate School of Kyushu University, Fukuoka 812-8581,JAPAN

Outline of the Subloading Surface Model with Tangential Stress Rate Effect

Let the stretching $\mathbf{D}$ be additively decomposed into the elastic stretching $\mathbf{D}^e$ and the inelastic stretching $\mathbf{D}^i$ which is further decomposed into the plastic stretching $\mathbf{D}^p$ and the tangential stretching $\mathbf{D}^t$, i.e.

$$\mathbf{D} = \mathbf{D}^e + \mathbf{D}^i, \qquad \mathbf{D}^i = \mathbf{D}^p + \mathbf{D}^t, \qquad \mathbf{D}^e = \mathbf{E}^{-1}\overset{\circ}{\boldsymbol{\sigma}}. \tag{1}$$

$\boldsymbol{\sigma}$ is the Cauchy stress and $(^{\circ})$ indicates the proper corotational rate with the objectivity and the fourth-order tensor $\mathbf{E}$ is the elastic modulus.

Now, let the *subloading surface* [1, 3] be introduced, which always passes through the current stress $\boldsymbol{\sigma}$ and keeps the similarity to the *normal-yield surface*. The subloading surface is given by

$$f(\overline{\boldsymbol{\sigma}}, \mathbf{H}) = RF(H), \qquad \overline{\boldsymbol{\sigma}} = \boldsymbol{\sigma} - \overline{\boldsymbol{\alpha}}, \qquad \overline{\boldsymbol{\alpha}} = \mathbf{s} - R(\mathbf{s} - \boldsymbol{\alpha}), \tag{2}$$

where the second-order tensor $\mathbf{H}$ and the scalar H are anisotropic and isotropic hardening variables, respectively. The second-order tensor $\boldsymbol{\alpha}$ is the reference point inside the normal-yield surface, which plays the role of the kinematic hardening variable as it translates with the plastic deformation. $\overline{\boldsymbol{\alpha}}$ in the subloading surface is the conjugate point of $\boldsymbol{\alpha}$. R $(0 \le R \le 1)$ is the ratio of size of the subloading surface to that of the normal-yield surface. $\mathbf{s}$ is the *similarity-center* of these surfaces. The translation rule of the similarity-center $\mathbf{s}$ is given by

$$\overset{\circ}{\mathbf{s}} = c_s \,\|\, \mathbf{D}^p \,\|\, \frac{\overset{\circ}{\overline{\boldsymbol{\sigma}}}}{R} + \overset{\circ}{\boldsymbol{\alpha}} + \frac{1}{F}\left\{ \overset{\circ}{F} - \mathrm{tr}\left(\frac{\partial f(\hat{\mathbf{s}}, \mathbf{H})}{\partial \mathbf{H}} \overset{\circ}{\mathbf{H}} \right) \right\} \hat{\mathbf{s}}, \qquad \overset{\circ}{\overline{\boldsymbol{\sigma}}} = \overset{\circ}{\boldsymbol{\sigma}} - \overset{\circ}{\mathbf{s}}, \qquad \hat{\mathbf{s}} \equiv \mathbf{s} - \boldsymbol{\alpha}. \tag{3}$$

where c_s is a material constant prescribing the translating rate of the similarity-center. $\|\ \|$ stands for the magnitude.

The evolution rule of R is given by

$$\overset{\circ}{R} = U \,\|\, \mathbf{D}^p \,\| \quad \text{for} \quad \mathbf{D}^p \neq 0, \qquad U = -u \ln R, \tag{4}$$

where u (> 0) is a material constant.

On the other hand, $\mathbf{D}^t$ in Eq. (1) is induced by the stress rate component tangential to the subloading surface. Thus, $\mathbf{D}^t$ is called the *tangential stretching*. Let the tangential stretching $\mathbf{D}^t$ be formulated as

$$\mathbf{D}^t = \frac{1}{T}\overset{\circ}{\boldsymbol{\sigma}}{}^*_t, \qquad T = \frac{\xi}{R^b}. \tag{5}$$

The function T is called the *tangential inelastic modulus*, where $b\,(\ge 1)$ is a material constant, ξ is the material function of stress and internal variables in general. The second-order tensor $\overset{\circ}{\boldsymbol{\sigma}}{}^*_t$, called the *deviatoric-tangential stress rate*, is given as follows:

$$\overset{\circ}{\boldsymbol{\sigma}}{}^{*}_{t} \equiv \overset{\circ}{\boldsymbol{\sigma}}{}^{*} - \overset{\circ}{\boldsymbol{\sigma}}{}^{*}_{n}, \quad \overset{\circ}{\boldsymbol{\sigma}}{}^{*}_{n} \equiv \mathrm{tr}(\bar{\mathbf{n}}^{*}\overset{\circ}{\boldsymbol{\sigma}}{}^{*})\bar{\mathbf{n}}^{*}, \quad \overset{\circ}{\boldsymbol{\sigma}}{}^{*} \equiv \overset{\circ}{\boldsymbol{\sigma}} - \overset{\circ}{\sigma}_{m}\mathbf{I}, \quad \sigma_{m} \equiv \frac{1}{3}\mathrm{tr}\boldsymbol{\sigma},$$

$$\bar{\mathbf{n}}^{*} \equiv \left(\frac{\partial f(\bar{\boldsymbol{\sigma}},\mathbf{H})}{\partial \boldsymbol{\sigma}}\right)^{*} \Bigg/ \left\| \left(\frac{\partial f(\bar{\boldsymbol{\sigma}},\mathbf{H})}{\partial \boldsymbol{\sigma}}\right)^{*} \right\| = \frac{\bar{\mathbf{N}}^{*}}{\| \bar{\mathbf{N}}^{*} \|} \quad (\|\bar{\mathbf{n}}^{*}\| = 1), \tag{6}$$

$$\bar{\mathbf{N}}^{*} \equiv \left(\frac{\partial f(\bar{\boldsymbol{\sigma}},\mathbf{H})}{\partial \boldsymbol{\sigma}}\right)^{*} \Bigg/ \left\| \left(\frac{\partial f(\bar{\boldsymbol{\sigma}},\mathbf{H})}{\partial \boldsymbol{\sigma}}\right) \right\|.$$

$(\,)^{*}$ stands for the deviatoric part.

Adopt the *associated flow rule*

$$\mathbf{D}^{p} = \lambda \bar{\mathbf{N}}, \quad \bar{\mathbf{N}} \equiv \frac{\partial f(\bar{\boldsymbol{\sigma}},\mathbf{H})}{\partial \boldsymbol{\sigma}} \Bigg/ \left\| \frac{\partial f(\bar{\boldsymbol{\sigma}},\mathbf{H})}{\partial \boldsymbol{\sigma}} \right\|, \tag{7}$$

where λ is the positive proportionality factor.

The stretching $\mathbf{D}$ is given from Eqs. (1) and (7) as

$$\mathbf{D} = \mathbf{E}^{-1}\overset{\circ}{\boldsymbol{\sigma}} + \frac{tr(\bar{\mathbf{N}}\overset{\circ}{\boldsymbol{\sigma}})}{\bar{M}_{p}}\bar{\mathbf{N}} + \frac{\overset{\circ}{\boldsymbol{\sigma}}{}^{*}_{t}}{T}, \tag{8}$$

where

$$\bar{M}_{p} \equiv \mathrm{tr}\left[\bar{\mathbf{N}}\left(\bar{\mathbf{a}} + \left\{\frac{F'}{F}h - \frac{1}{RF}\mathrm{tr}\left(\frac{\partial f(\bar{\boldsymbol{\sigma}},\,\mathbf{H})}{\partial \mathbf{H}}\mathbf{h}\right) + \frac{U}{R}\right\}\bar{\boldsymbol{\sigma}}\right)\right], \tag{9}$$

$$h \equiv \frac{\overset{\circ}{H}}{\lambda}, \qquad \mathbf{h} \equiv \frac{\overset{\circ}{\mathbf{H}}}{\lambda}, \qquad \bar{\mathbf{a}} \equiv \frac{\overset{\circ}{\bar{\boldsymbol{\alpha}}}}{\lambda} = R\mathbf{a} + (1-R)\mathbf{z} - U\hat{\mathbf{s}},$$

$$\mathbf{a} \equiv \frac{\overset{\circ}{\boldsymbol{\alpha}}}{\lambda}, \qquad \mathbf{z} \equiv \frac{\overset{\circ}{\mathbf{s}}}{\lambda} = c\frac{\overset{\circ}{\boldsymbol{\sigma}}}{R} + \mathbf{a} + \frac{1}{F}\left\{F'h - \mathrm{tr}\left(\frac{\partial f(\hat{\mathbf{s}},\mathbf{H})}{\partial \mathbf{H}}\mathbf{h}\right)\right\}\hat{\mathbf{s}}$$

The loading criterion is given as follows:

$$\left.\begin{aligned} &\mathbf{D}^{p} \neq 0 : \mathrm{tr}(\bar{\mathbf{N}}\mathbf{E}\mathbf{D}) > 0, \\ &\mathbf{D}^{p} = 0 : \mathrm{tr}(\bar{\mathbf{N}}\mathbf{E}\mathbf{D}) \leq 0. \end{aligned}\right\} \tag{10}$$

Material Function for Soils

Let the stress function $f(\bar{\boldsymbol{\sigma}},\mathbf{H})$ for soils be given as

$$f(\bar{\boldsymbol{\sigma}},\mathbf{H}) = \bar{p}(1+\bar{\chi}^2), \qquad \bar{p} \equiv -\frac{1}{3}\mathrm{tr}\bar{\boldsymbol{\sigma}}, \quad \bar{\chi} \equiv \frac{\|\bar{\boldsymbol{\eta}}\|}{\bar{m}}, \quad \bar{\boldsymbol{\eta}} \equiv \bar{\mathbf{Q}} - \boldsymbol{\beta}, \quad \bar{\mathbf{Q}} \equiv \frac{\bar{\boldsymbol{\sigma}}^*}{\bar{p}}, \tag{11}$$

$$\bar{\boldsymbol{\sigma}}^* = \bar{\boldsymbol{\sigma}} + \bar{p}\mathbf{I}, \quad \bar{m} = \frac{14\sqrt{6}\sin\phi}{(3-\sin\phi)(8-\sin 3\bar{\theta}_\eta)}, \quad \sin 3\bar{\theta}_\eta \equiv -\sqrt{6}\frac{\mathrm{tr}\bar{\boldsymbol{\eta}}^3}{\|\bar{\boldsymbol{\eta}}\|^3}, \tag{12}$$

where ϕ is the material constant. The anisotropic hardening variable $\mathbf{H}$ is selected as the rotational hardening variable $\boldsymbol{\beta}$. The evolution rule of rotational hardening is given by

$$\overset{\circ}{\boldsymbol{\beta}} = b_r \left\| \mathbf{D}^{p*} \right\| \|\bar{\boldsymbol{\eta}}\| \bar{\boldsymbol{\eta}}_b, \qquad \bar{\boldsymbol{\eta}}_b \equiv \bar{m}_b \bar{\mathbf{t}} - \boldsymbol{\beta}, \quad \bar{\mathbf{t}} \equiv \frac{\bar{\boldsymbol{\eta}}}{\|\bar{\boldsymbol{\eta}}\|}, \quad \bar{m}_b = \frac{14\sqrt{6}\sin\phi_b}{(3-\sin\phi_b)(8-\sin 3\bar{\theta}_\eta)}, \tag{13}$$

where b_r and ϕ_b are material constants. The isotropic hardening/softening variable H for sands as follows:

$$\overset{\circ}{H} = -D_v^p + \mu \left\| \mathbf{D}^{p*} \right\| (\|\bar{\boldsymbol{\eta}}\| - \bar{m}_d),$$
$$\bar{m}_d = \frac{14\sqrt{6}\sin\phi_d}{(3-\sin\phi_d)(8-\sin 3\bar{\theta}_\sigma)}, \quad \sin 3\bar{\theta}_\sigma \equiv -\sqrt{6}\frac{\mathrm{tr}\boldsymbol{\sigma}^{*3}}{\|\boldsymbol{\sigma}^*\|^3}, \tag{14}$$

where μ and ϕ_d are material constants. The isotropic hardening function F is given by

$$F = F_0 \exp\{H/(\rho - \gamma)\}. \tag{15}$$

F_0 is initial value of F and ρ and γ are material constants. The function ξ in the tangential inelastic modulus T of Eq. (5) is given by

$$\xi = \frac{p}{a\bar{\chi}^c} \tag{16}$$

a and c (≥ 1) are material constants.

Simulation and Discussions

The validity of the above-mentioned constitutive equation is examined by the simulation for the test data of Hostun sand under the drained condition [4]. The coordinate system $(x_1, x_2, x_3,)$ is taken for the true triaxial test apparatus as shown in Fig.1 where $\sigma_1, \sigma_2, \sigma_3$ are principal stresses, $\varepsilon_1, \varepsilon_2, \varepsilon_3$ are calculated by the time integration of the three principal stretching D_1, D_2, D_3.

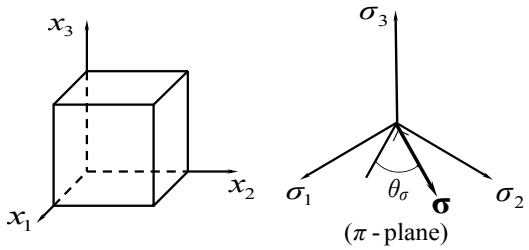

Fig.1. Coordinate system for the true triaxial test apparatus.

This test is split into two stages: I) The axial stress σ_3 was decreased by –343 to –843kPa from the isotropic stress state of –500kPa, while σ_1 and σ_2 were both increased proportionately by 171 to –329kPa, keeping the mean stress σ_m at –500kPa. The magnitude of deviatoric stress $\|\boldsymbol{\sigma}^*\|$ finally became 420kPa. II) A circular stress path (θ_σ =30→750°) in two cycles was traced in a deviatoric stress plane by varying three principal stresses $\sigma_1, \sigma_2, \sigma_3$ in sinusoidal forms, σ_m and $\|\boldsymbol{\sigma}^*\|$ being kept to be constant. The following initial values and material constants are used in the calculation.

$$\boldsymbol{\sigma}_0 = -100\mathbf{I}\ \text{kPa},\ \ F_0 = 540\ \text{kPa},\ \ \mathbf{s}_0 = 7\ \text{kPa},\ \ \phi = 27.7°\ \ \rho = 0.007,\ \ \gamma = 0.003,$$
$$u = 20,\ \ \nu = 0.3,\ \ c_s = 5,\ \ \phi_b = 25°,\ \ br = 95,\ \ \phi_d = 32°,\ \ \mu = 0.9,\ \ a = 0.009,\ \ b = 2.2,\ \ c = 1$$

The predicted and tested principal strains $\varepsilon_1, \varepsilon_2, \varepsilon_3$ and the volumetric strain ε_v vs. the angle θ_σ are shown in Fig. 2. Variations of principal and volumetric strains are predicted well in both the first (θ_σ =30→390°) and second (θ_σ =390→750°) circular stress path.

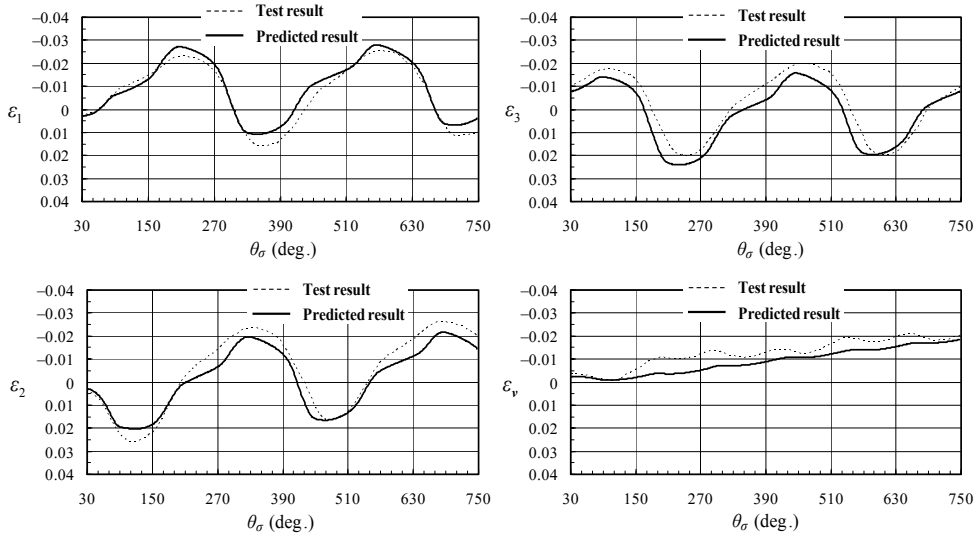

Fig. 2. Variations of three principal strain $\varepsilon_1, \varepsilon_2, \varepsilon_3$ and volumetric strain ε_v vs. θ_σ for the cyclic loading of circular stress path in the π - plane.

The strain paths in the π–plane calculated by the elastic, plastic and tangential stretching are shown in Fig. 3. The direction of the elastic stretching coincides with the stress rate and then the strain path exhibits the circular shape. The strain path due to the plastic stretching exhibits the shape of two triangles such that the subloading surface in the π-plane rotated $\pi/2$ in the clockwise rotation because the plastic stretching occurs perpendicular to the subloading surface according to the associated flow rule. The direction of the tangent stretching is induced by the deviatoric stress rate tangential to the subloading surface and then the strain path exhibits the similar shape of the subloading surface in the π-plane. It is also observed in the figure that the tangential stretching is induced always depending on the normal-yield ratio R.

The predicted strain path in the π-plane is shown in Fig.4 comparing with the test result. It is observed that the simulation is improved by incorporating the tangential stretching $\mathbf{D}^t$. Thus, the subloading surface model with the tangential stress rate effect can describe realistically the deformation behavior of the soil in a loading process deviating significantly from the proportional loading.

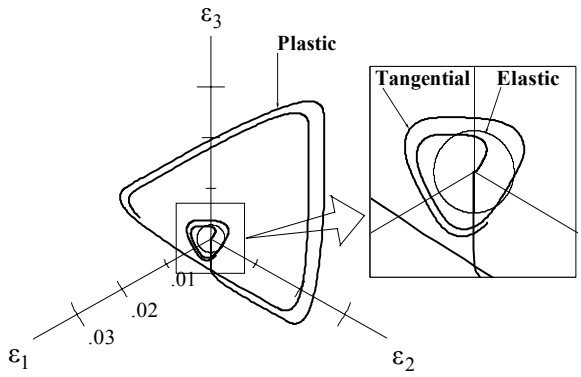

Fig. 3. Elastic, plastic and tagential strain paths in the π - plane.

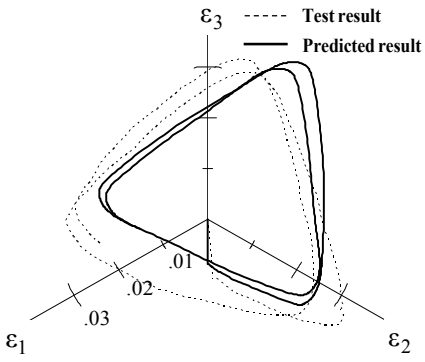

Fig. 4. Strain path in the π - plane.

Reference

1. Hashiguchi, K. and Ueno, M. (1977): Elastoplastic constitutive laws of granular materials, *Constitutive Equations of Soils* (*Proc. 9th Int. Conf. Soil Mech. Found. Eng., Spec. Session 9, Tokyo*), JSSMFE, pp.73-82.

2. Hashiguchi, K. and Tsutsumi, S. (2001): Elastoplastic constitutive equation with tangential stress rate effect, *Int. J. Plasticity*, Vol.17, pp.117-145.

3. Hashiguchi, K. (1989): Subloading surface model in unconventional plasticity, *Int. J. Solids Struct.*, 25, pp.917-945.

4. A. S. Saada and G. Bianchini (eds.) (1989): *Proc. Int. Workshop on Constitutive Equations for Granular Non-cohesive Soils*, Cleveland, Balkema, Rotterdam.